11

CONTROLLING CHAOS IN MECHANICAL SYSTEMS

ERNEST BARRETO, YING-CHENG LAI, and CELSO GREBOGI

11.1 INTRODUCTION

The control of chaos by unstable periodic orbits embedded in a chaotic attractor was first proosed in 1990 (Ott, Grebogi, and Yorke, 1990). Numerous experiments in many different fields have demonstrated the feasibility of this approach. This technique has been applied for example to mechanical systems (Ditto, Rauseo, and Spano, 1990; Hübinger et al., 1994; Starrett and Tagg, 1994; Moon, Johnson, and Holmes, 1996), lasers (Roy et al., 1992; Gills et al., 1992; Bielawski, et al., 1993, 1994; Reyl et al., 1993; Meucci et al., 1994), circuits (Hunt, 1991; Johnson and Hunt, 1993; Gauthier et al., 1994), chemical reactions (Petrov et al., 1993, 1994), biological systems (Schiff et al., 1994; Garfinkel et al., 1992), communication technology (Hayes, Grebogi, and Ott, 1993; Hayes et al., 1994), and energy production methods (Rhode et al., 1995; Daw et al., 1995). Furthermore it is possible to switch efficiently from one unstable periodic orbit to another at will (Ditto, Rauseo, and Spano, 1990; Romeiras et al., 1992; Kostelich et al., 1993; Barreto et al., 1995a). The basic idea is as follows: First, one chooses an unstable periodic orbit embedded in an attractor that yields the best system performance according to some criteria. Second one allows the trajectory to enter a small region around the desired

Dynamics and Chaos in Manufacturing Processes, Edited by Francis C. Moon.
ISBN 0-471-15293-5

orbit, which is bound to happen because of the ergodicity of the chaotic attractor. As this occurs, small, judiciously chosen parameter perturbations are applied to force the trajectory to approach the unstable periodic orbit. This method is extremely flexible because chaotic attractors typically have embedded within them an infinite number of unstable periodic orbits. Thus, by choosing a set of system parameters that yields chaos, one has access to a great many different system behaviors.

In this chapter, we illustrate the idea of controlling chaos using both low- and high-dimensional dynamical systems. As a pedagogic example, in Section 11.2 we use the logistic map to elucidate the fundamental concepts and methodology. In Section 11.3 we emphasize the geometrically intuitive two-dimensional case and present a general algorithm applicable to systems of any dimension. In Section 11.4 we present an application to a mechanical system, the kicked double rotor. We also discuss a method for rapidly steering chaotic trajectories to a desirable periodic orbit on the attractor. We draw our conclusions in Section 11.5.

11.2 A ONE-DIMENSIONAL EXAMPLE

The basic idea behind controlling chaos can be understood by considering a simple model system. We consider one of the best understood chaotic systems, the simple one-dimensional logistic map:

$$x_{n+1} = f(x_n, \lambda) = \lambda x_n(1 - x_n), \tag{1}$$

where x is restricted to the unit interval $[0, 1]$ and λ is a control parameter. It is known that this map develops chaos via the period-doubling bifurcation route (Feigenbaum, 1978). For $0 < \lambda < 1$, the asymptotic state of the map (or the attractor of the map) is $x = 0$; for $1 < \lambda < 3$, the attractor is a nonzero fixed point $x_F = 1 - 1/\lambda$; for $3 < \lambda < 1 + \sqrt{6}$, this fixed point is unstable and the attractor is a stable period-2 orbit. As λ is increased further, a sequence of period-doubling bifurcations occurs in which successive period-doubled orbits become stable. The period-doubling cascade accumulates at $\lambda = \lambda_\infty \approx 3.57$, after which chaos arises.

Consider the case $\lambda = 3.8$ shown in Figure 11.1*a* where the system is apparently chaotic. An important characteristic of a chaotic attractor is that there exists *an infinite number of unstable periodic orbits embedded within it.* Shown in the figure are, for example, a fixed point $x_F \approx 0.7368$ and a period-2 orbit with components $x(1) \approx 0.3737$ and $x(2) \approx 0.8894$, where $x(1) = f(x(2))$ and $x(2) = f(x(1))$.

Suppose that we want to avoid chaos at $\lambda = 3.8$. In particular, we want trajectories resulting from a randomly chosen initial condition x_0 to be as close as possible to the period-2 orbit shown in Figure 11.1*a*, assuming that this

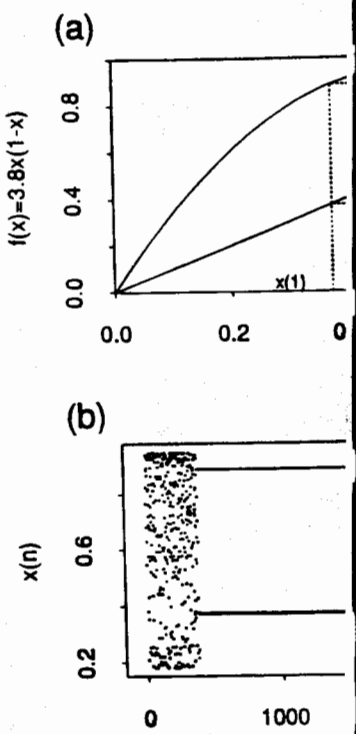

FIGURE 11.1. (*a*) The logistic map $x_$ point and an unstable period-2 orbit a control of the period-2 orbit and the fi $x_0 = 0.28$. At $n = 381$, the trajectory fa after which the parameter control is tu period-2 orbit. At $n = 2200$, the control comes close to the fixed point and is c $\varepsilon = 10^{-3}$. The maximum allowed paran

period-2 orbit gives the best system desired asymptotic state of the map periodic orbits. Suppose further th small range around the value $\lambda_0 =$ $[\lambda_0 - \delta, \lambda_0 + \delta]$, where $\delta \ll 1$. Due trajectory that begins from an arbi one, into the neighborhood of the Because of the nature of chaos, the period-2 orbit if we do not interver the control parameter so that the t

e of the ergodicity of the chaotic
chosen parameter perturbations are
h the unstable periodic orbit. This
ic attractors typically have embed-
unstable periodic orbits. Thus, by
elds chaos, one has access to a great

controlling chaos using both low-
As a pedagogic example, in Section
te the fundamental concepts and
ze the geometrically intuitive two-
orithm applicable to systems of any
pplication to a mechanical system,
method for rapidly steering chaotic
on the attractor. We draw our

LE

an be understood by considering a
ne best understood chaotic systems,

$$x_n(1 - x_n), \qquad (1)$$

1] and λ is a control parameter. It
ia the period-doubling bifurcation
he asymptotic state of the map (or
< 3, the attractor is a nonzero fixed
nis fixed point is unstable and the
is increased further, a sequence of
ch successive period-doubled orbits
ide accumulates at $\lambda = \lambda_\infty \approx 3.57$,

Figure 11.1*a* where the system is
ristic of a chaotic attractor is that
periodic orbits embedded within it.
d point $x_F \approx 0.7368$ and a period-2
$(2) \approx 0.8894$, where $x(1) = f(x(2))$

at $\lambda = 3.8$. In particular, we want
en initial condition x_0 to be as close
n Figure 11.1*a*, assuming that this

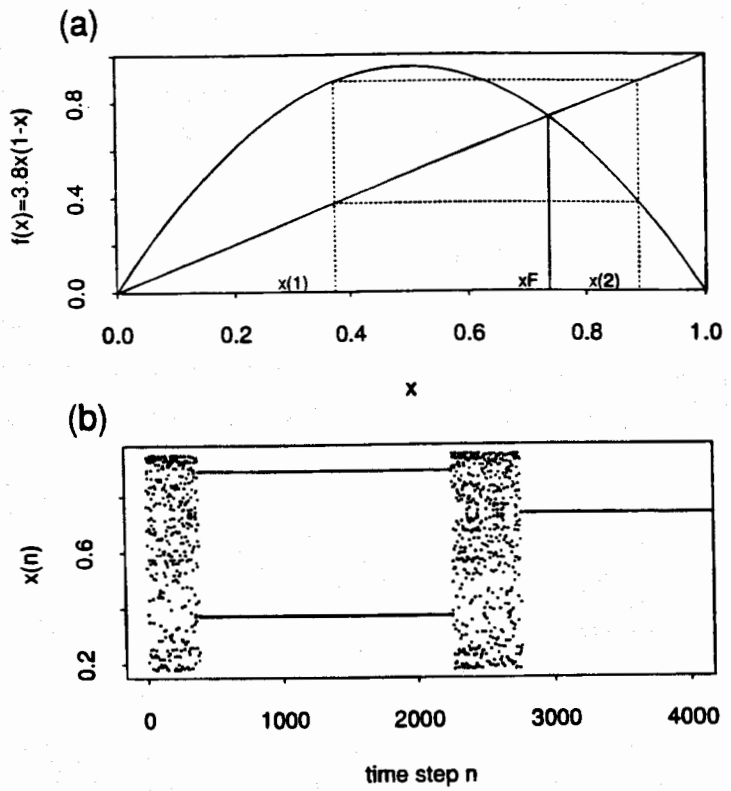

FIGURE 11.1. (*a*) The logistic map $x_{n+1} = f(x_n) = 3.8x_n(1 - x_n)$. An unstable fixed point and an unstable period-2 orbit are also shown. (*b*) Time series illustrating the control of the period-2 orbit and the fixed point. The chaotic trajectory begins from $x_0 = 0.28$. At $n = 381$, the trajectory falls in an ε-neighborhood of the period-2 orbit, after which the parameter control is turned on to stabilize the trajectory around the period-2 orbit. At $n = 2200$, the control is turned off. At $n = 2757$, the chaotic trajectory comes close to the fixed point and is controlled in subsequent iterations. We choose $\varepsilon = 10^{-3}$. The maximum allowed parameter perturbation is $\delta = 5 \times 10^{-3}$.

period-2 orbit gives the best system performance. Of course we can choose the desired asymptotic state of the map to be any of the infinite number of unstable periodic orbits. Suppose further that the parameter λ can be fine-tuned in a small range around the value $\lambda_0 = 3.8$, namely we allow λ to vary in the range $[\lambda_0 - \delta, \lambda_0 + \delta]$, where $\delta \ll 1$. Due to the nature of the chaotic attractor, a trajectory that begins from an arbitrary value of x_0 will fall, with probability one, into the neighborhood of the desired period-2 orbit at some later time. Because of the nature of chaos, the trajectory would diverge quickly from the period-2 orbit if we do not intervene. Our task is to program the variation of the control parameter so that the trajectory stays in the neighborhood of the

period-2 orbit as long as the control is present. In general, the small parameter perturbations will be time dependent. We emphasize that it is important to apply only small parameter perturbations. If large parameter perturbations are allowed, then obviously we can eliminate chaos by varying λ from 3.8 to 2.0, for example. Such a large change is not interesting.

The logistic map in the neighborhood of a periodic orbit can be approximated by a linear equation expanded around the periodic orbit. Denote the target period-m orbit to be controlled as $x(i)$, $i = 1,\ldots, m$, where $x(i+1) = f(x(i))$ and $x(m+1) = x(1)$. Assume that at time n the trajectory falls into the neighborhood of component i of the period-m orbit. The linearized dynamics in the neighborhood of component $i+1$ is then

$$x_{n+1} - x(i+1) = \frac{\partial f}{\partial x}[x_n - x(i)] + \frac{\partial f}{\partial \lambda}\Delta\lambda_n$$
$$= \lambda_0[1 - 2x(i)][x_n - x(i)] + x(i)[1 - x(i)]\Delta\lambda_n, \qquad (2)$$

where the partial derivatives in (2) are evaluated at $x = x(i)$ and $\lambda = \lambda_0$. We require x_{n+1} to stay in the neighborhood of $x(i+1)$. Hence we set $x_{n+1} - x(i+1) = 0$, which gives

$$\Delta\lambda_n = \lambda_0 \frac{[2x(i) - 1][x_n - x(i)]}{x(i)[1 - x(i)]}. \qquad (3)$$

Equation (3) holds only when the trajectory x_n enters a small neighborhood of the period-m orbit, namely when $|x_n - x(i)| \ll 1$; hence the required parameter perturbation $\Delta\lambda_n$ is small. Let the length of a small interval defining the neighborhood around each component of the period-m orbit be 2ε. In general, the required maximum parameter perturbation δ is proportional to ε. Since ε can be chosen to be arbitrarily small, δ also can be made arbitrarily small. As we will see, the average transient time before a trajectory enters the neighborhood of the target periodic orbit depends on ε (or δ). When the trajectory is outside the neighborhood of the target periodic orbit, we do not apply any parameter perturbation, and the system evolves at its nominal parameter value λ_0. Hence we usually set $\Delta\lambda_n = 0$ when $\Delta\lambda_n > \delta$. Note that the parameter perturbation $\Delta\lambda_n$ depends on x_n and is time dependent.

The above strategy for controlling the orbit is very flexible for stabilizing different periodic orbits at different times. Suppose that we first stabilize a chaotic trajectory around the period-2 orbit shown in Figure 11.1*a*. Then we might wish to stabilize the fixed point in Figure 11.1*a*, assuming that the fixed point would correspond to a better system performance at a later time. To achieve this change of control, we simply turn off the parameter control with respect to the period-2 orbit. Without control, the trajectory will diverge from the period-2 orbit exponentially. We let the system evolve at the parameter value λ_0. Due to the nature of chaos, there comes a time when the chaotic

trajectory enters a small neighborho
on a new set of parameter perturbe
point. The trajectory can then be st

Figure 11.1*b* shows an example w
then the fixed point shown in Figur
At time $n = 381$, the trajectory ente
the period-2 orbit. For subsequent i
from (3) is used to stabilize the traj
$n = 2200$, we chose to stabilize the tr
we turn off the parameter perturb
period-2 orbit and becomes chaotic.
the neighborhood of the fixed point
respect to the fixed point are then tu
the fixed point.

In the presence of external noise,
"kicked" out of the neighborhood of
we turn off the parameter perturbati
probability one the chaotic trajector
periodic orbit and be controlled ag
11.2*a* where we control the period-2
term in the logistic map of the forr
random variable with zero mean and
amplitude. The effect of the noise is t
an intermittent one in which chao
interspersed with laminar phases (cc
verify that the averaged length of
amplitude decreases, and the length

Let us consider how many iterat
trajectory originating from an arbit
neighborhood ε of the target period
the more iterations are required. I
before turning on control scales wit

$$\tau(\varepsilon$$

where $\gamma > 0$ is a scaling exponent.
logistic map, there usually exists
trajectory points on the attractor. T
the frequency that a chaotic trajecto
x on the attractor. In such a case we
argument: The probability that a
particular component (component i

$$P(\varepsilon) = \int_{x(i)-\varepsilon}^{x(i)+\varepsilon}$$

nt. In general, the small parameter
emphasize that it is important to
large parameter perturbations are
naos by varying λ from 3.8 to 2.0,
resting.

f a periodic orbit can be approxi-
nd the periodic orbit. Denote the
(i), $i = 1, \ldots, m$, where $x(i+1) =$
time n the trajectory falls into the
-m orbit. The linearized dynamics
then

$$\frac{f}{\lambda}\Delta\lambda_n$$

$$- x(i)] + x(i)[1 - x(i)]\Delta\lambda_n, \qquad (2)$$

luated at $x = x(i)$ and $\lambda = \lambda_0$. We
ood of $x(i+1)$. Hence we set

$$\frac{[x_n - x(i)]}{- x(i)]}. \qquad (3)$$

ory x_n enters a small neighborhood
$x(i)| \ll 1$; hence the required par-
gth of a small interval defining the
he period-m orbit be 2ε. In general,
tion δ is proportional to ε. Since ε
can be made arbitrarily small. As
e a trajectory enters the neighbor-
on ε (or δ). When the trajectory is
riodic orbit, we do not apply any
lves at its nominal parameter value
$\Delta\lambda_n > \delta$. Note that the parameter
dependent.

orbit is very flexible for stabilizing
Suppose that we first stabilize a
t shown in Figure 11.1*a*. Then we
gure 11.1*a*, assuming that the fixed
n performance at a later time. To
urn off the parameter control with
ol, the trajectory will diverge from
e system evolve at the parameter
e comes a time when the chaotic

trajectory enters a small neighborhood of the fixed point. At this time we turn on a new set of parameter perturbations calculated with respect to the fixed point. The trajectory can then be stabilized around the fixed point.

Figure 11.1*b* shows an example where we first control the period-2 orbit and then the fixed point shown in Figure 11.1*a*. The initial condition is $x_0 = 0.28$. At time $n = 381$, the trajectory enters the neighborhood of component $x(1)$ of the period-2 orbit. For subsequent iterations the parameter control calculated from (3) is used to stabilize the trajectory around the period-2 orbit. At time $n = 2200$, we chose to stabilize the trajectory around the fixed point, and hence we turn off the parameter perturbation. The trajectory quickly leaves the period-2 orbit and becomes chaotic. At time $n = 2757$, the trajectory falls into the neighborhood of the fixed point. Parameter perturbations calculated with respect to the fixed point are then turned on to stabilize the trajectory around the fixed point.

In the presence of external noise, a controlled trajectory will occasionally be "kicked" out of the neighborhood of the periodic orbit. If this behavior occurs, we turn off the parameter perturbation and let the system evolve by itself. With probability one the chaotic trajectory will enter the neighborhood of the target periodic orbit and be controlled again. This situation is illustrated in Figure 11.2*a* where we control the period-2 orbit. The noise is modeled by an additive term in the logistic map of the form $\eta\sigma_n$, where σ_n is a Gaussian distributed random variable with zero mean and unit standard deviation, and η is the noise amplitude. The effect of the noise is to turn a controlled periodic trajectory into an intermittent one in which chaotic phases (uncontrolled trajectories) are interspersed with laminar phases (controlled periodic trajectories). It is easy to verify that the averaged length of the laminar phase increases as the noise amplitude decreases, and the length tends to infinity as $\eta \to 0$.

Let us consider how many iterations are required on average for a chaotic trajectory originating from an arbitrarily chosen initial condition to enter the neighborhood ε of the target periodic orbit. Clearly the smaller the value of ε, the more iterations are required. In general, the average transient time $\tau(\varepsilon)$ before turning on control scales with ε as

$$\tau(\varepsilon) \sim \varepsilon^{-\gamma}, \qquad (4)$$

where $\gamma > 0$ is a scaling exponent. For one-dimensional maps such as the logistic map, there usually exists a smooth probability density $\rho(x)$ for trajectory points on the attractor. The probability density ρ can be defined as the frequency that a chaotic trajectory visits a small neighborhood of the point x on the attractor. In such a case we have $\gamma = 1$, as can be seen by the following argument: The probability that a trajectory enters the neighborhood of a particular component (component i) of the periodic orbit is given by

$$P(\varepsilon) = \int_{x(i)-\varepsilon}^{x(i)+\varepsilon} \rho(x(i))dx \approx 2\varepsilon\rho(x(i)). \qquad (5)$$

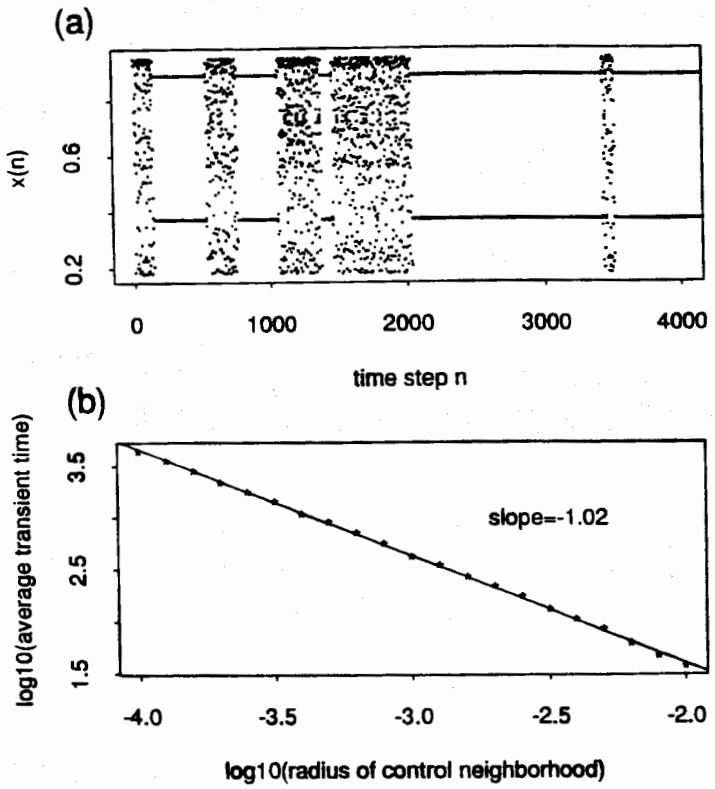

FIGURE 11.2. (*a*) The effect of additive noise modeled by $2.6 \times 10^{-4}\sigma_n$, where σ_n is a Gaussian random variable with zero mean and unit standard deviation. The noise can occasionally kick the controlled trajectory out of the neighborhood of the periodic orbit. (*b*) Log-log plot of the average time to achieve control $\tau(\varepsilon)$ versus ε, the size of the controlling neighborhood. Twenty values of ε are chosen on a logarithmic scale. For each ε, 2000 random initial conditions uniformly distributed in $[0, 1]$ are chosen to compute $\tau(\varepsilon)$. The scaling relation between $\tau(\varepsilon)$ and ε is well fitted by $\tau(\varepsilon) \sim \varepsilon^{-1}$.

Hence $\tau(\varepsilon) = 1/P(\varepsilon) \sim \varepsilon^{-1}$, and therefore $\gamma = 1$. This behavior is illustrated in Figure 11.2*b*, where $\tau(\varepsilon)$ is plotted on a logarithmic scale for the case of stabilizing the period-2 orbit in Figure 11.1*a*. Twenty values of ε were chosen in the range $[10^{-4}, 10^{-2}]$. For each ε we randomly choose 2000 initial conditions (with a uniform probability distribution) and calculate an average transient time. The slope of the straight line is approximately -1.02, indicating good agreement with the theoretical prediction of $\gamma = 1$. For higher-dimensional chaotic systems, the exponent γ can be related to the eigenvalues of the target periodic orbit (Ott, Grebogi, and Yorke, 1990).

A major advantage of the controlling chaos idea is that it can be applied to experimental systems in which a priori knowledge of the system is usually not

known. A time series found by m
variables in conjunction with the
Casdagli, and Yorke, 1991; Ott, 19
into a trajectory in phase space, is s
periodic orbits to be controlled and t
parameter perturbations (Ditto, Ra
1992; Dressler and Nitsche, 1992; So
method is its flexibility in choosing t
The method has attracted growing
and has been extended to higher-din
al., 1992; Auerbach et al., 1992), Han
1993a), the control of transient cha
Tél, and Grebogi, 1993c) and the sy
Grebogi, 1993, 1994b). It also has
physical experiments (Ditto, Rauseo
In Section 11.3 we will describe the
maps.

11.3 CONTROLLING HIGHER

The general algorithm for controlli
autonomous flows that can be rec
section) can be formulated as follow
vector field does not contain an
d-dimensional map,

$$\mathbf{X}_{n+1}$$

where $\mathbf{X}_n \in \mathbf{R}^d$, $\mathbf{F}$ is a smooth functic
r externally accessible control paran
tions to be small, namely

$$|p^i - p_0^i| <$$

where $\mathbf{p}_0$ is some nominal parame
parameter variation. We wish to pr
trajectory is stabilized when it ent
odic orbit. Let the desired perioc
$\mathbf{X}(m, \mathbf{p}_0) \to \mathbf{X}(m + 1, \mathbf{p}_0) = \mathbf{X}(1, \mathbf{p}_0)$.
hood of component $i + 1$ of the per

$$\mathbf{X}_{n+1} - \mathbf{X}(i + 1, \mathbf{p}_0) =$$

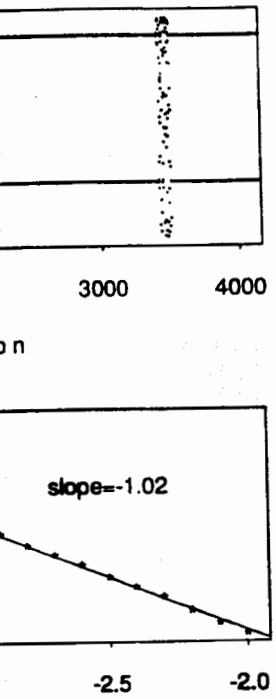

odeled by $2.6 \times 10^{-4}\sigma_n$, where σ_n is a unit standard deviation. The noise can of the neighborhood of the periodic hieve control $\tau(\varepsilon)$ versus ε, the size of are chosen on a logarithmic scale. For ly distributed in $[0, 1]$ are chosen to nd ε is well fitted by $\tau(\varepsilon) \sim \varepsilon^{-1}$.

$= 1$. This behavior is illustrated in logarithmic scale for the case of a. Twenty values of ε were chosen we randomly choose 2000 initial ribution) and calculate an average is approximately -1.02, indicating ction of $\gamma = 1$. For higher-dimen- be related to the eigenvalues of the rke, 1990).

ios idea is that it can be applied to wledge of the system is usually not

known. A time series found by measuring one of the system's dynamical variables in conjunction with the time delay embedding method (Sauer, Casdagli, and Yorke, 1991; Ott, 1993), which transforms a scalar time series into a trajectory in phase space, is sufficient to determine the desired unstable periodic orbits to be controlled and the relevant quantities required to compute parameter perturbations (Ditto, Rauseo, and Spano, 1990; Garfinkel et al., 1992; Dressler and Nitsche, 1992; So and Ott, 1995). Another advantage of the method is its flexibility in choosing the desired periodic orbit to be controlled. The method has attracted growing interest in controlling dynamical systems and has been extended to higher-dimensional dynamical systems (Romeiras et al., 1992; Auerbach et al., 1992), Hamiltonian systems (Lai, Ding, and Grebogi, 1993a), the control of transient chaos (Tél, 1991) and chaotic scattering (Lai, Tél, and Grebogi, 1993c) and the synchronization of chaotic systems (Lai and Grebogi, 1993, 1994b). It also has been successfully implemented in various physical experiments (Ditto, Rauseo, and Spano, 1990; Garfinkel et al., 1992). In Section 11.3 we will describe the method formulated for two-dimensional maps.

11.3 CONTROLLING HIGHER-DIMENSIONAL SYSTEMS

The general algorithm for controlling chaos in higher-dimensional maps (or autonomous flows that can be reduced to maps on a Poincaré surface of section) can be formulated as follows. (By autonomous flow we mean that the vector field does not contain an explicit time dependence.) Consider the d-dimensional map,

$$\mathbf{X}_{n+1} = \mathbf{F}(\mathbf{X}_n, \mathbf{p}) \tag{6}$$

where $\mathbf{X}_n \in \mathbf{R}^d$, $\mathbf{F}$ is a smooth function of its variables, and $\mathbf{p} \in \mathbf{R}^r$ is a vector of r externally accessible control parameters. We restrict the parameter perturbations to be small, namely

$$|p^i - p_0^i| < \delta_i, \qquad i = 1, \ldots, r, \tag{7}$$

where $\mathbf{p}_0$ is some nominal parameter value and $\delta_i \ll 1$ defines the range of parameter variation. We wish to program the parameters $\mathbf{p}$ so that a chaotic trajectory is stabilized when it enters an ε neighborhood of the target periodic orbit. Let the desired period-m orbit be $\mathbf{X}(1, \mathbf{p}_0) \to \mathbf{X}(2, \mathbf{p}_0) \to \cdots \to \mathbf{X}(m, \mathbf{p}_0) \to \mathbf{X}(m + 1, \mathbf{p}_0) = \mathbf{X}(1, \mathbf{p}_0)$. The linearized dynamics in the neighborhood of component $i + 1$ of the period-m orbit is

$$\mathbf{X}_{n+1} - \mathbf{X}(i + 1, \mathbf{p}_0) = \mathbf{A} \cdot [\mathbf{X}_n - \mathbf{X}(i, \mathbf{p}_0)] + \mathbf{B}\Delta\mathbf{p}_n, \tag{8}$$

where $\Delta\mathbf{p}_n = \mathbf{p}_n - \mathbf{p}_0$, $\mathbf{A}$ is a $d \times d$ Jacobian matrix, and $\mathbf{B}$ is a $d \times r$ matrix:

$$\mathbf{A} = \mathbf{D}_x\mathbf{F}(\mathbf{X}, \mathbf{p})_{|\mathbf{X}(i), \mathbf{p}_0},$$
$$\mathbf{B} = \mathbf{D}_\mathbf{p}\mathbf{F}(\mathbf{X}, \mathbf{p})_{|\mathbf{X}(i), \mathbf{p}_0}. \tag{9}$$

Now writing $\Delta\mathbf{p}_n = -\mathbf{K}\cdot[\mathbf{X}_n - \mathbf{X}(i, \mathbf{p}_0)]$, we have

$$\mathbf{X}_{n+1} - \mathbf{X}(i+1, \mathbf{p}_0) = [\mathbf{A} - \mathbf{BK}]\cdot[\mathbf{X}_n - \mathbf{X}(i, \mathbf{p}_0)]. \tag{10}$$

For a *controllable* system, standard techniques allow us to find a matrix $\mathbf{K}$ such that $[\mathbf{A} - \mathbf{BK}]$ has any desired eigenvalues. (The controllability condition and the construction of the matrix $\mathbf{K}$ are described in Barreto and Grebogi, 1995b, and Ogata, 1987.) By selecting eigenvalues of magnitude less than one, $\mathbf{X}_n - \mathbf{X}(i, \mathbf{p}_0)$ approaches 0.

The formulation above assumes that the complete state of the system $\mathbf{X}_n$ is known at any every map iteration. In practice, this is unrealistic. The method can, however, be implemented by measuring a single scalar time series via the embedding technique (Sauer, Casdagli, and Yorke, 1991; Ott, 1993). We refer the interested reader to Ditto, Rauseo, and Spano (1990) and Garfinkel et al., (1992) for further information.

We now emphasize the geometrical aspects of the higher-dimensional algorithm by discussing the two-dimensional case. (We further simplify the discussion by assuming only one control parameter.) A key aspect of higher-dimensional maps is that there exist both stable and unstable directions at each component of an unstable periodic orbit. The stable (unstable) directions are directions along which points approach (leave) the periodic orbit exponentially. The existence of this structure at each point of the trajectory can be seen for the two-dimensional case as follows: Choose a small circle of radius ε around an orbit point $\mathbf{X}(i)$. This circle can be written as $dx^2 + dy^2 = \varepsilon^2$ in the Cartesian coordinate system whose origin is at $\mathbf{X}(i)$. The image of the circle under $\mathbf{F}^{-1}$ can be expressed as $Adx'^2 + Bdx'dy' + Cdy'^2 = 1$, an equation for an ellipse in the Cartesian coordinate system whose origin is at $\mathbf{X}(i-1)$. The coefficients A, B, and C are functions of elements of the inverse Jacobian matrix at $\mathbf{X}(i)$. This deformation from a circle to an ellipse means that the distance along the major axis of the ellipse at $\mathbf{X}(i-1)$ contracts as a result of the map. Similarly the image of a circle at $\mathbf{X}(i-1)$ under $\mathbf{F}$ is typically an ellipse at $\mathbf{X}(i)$, which means that the distance along the inverse image of the major axis of the ellipse at $\mathbf{X}(i)$ expands under $\mathbf{F}$. Thus the major axis of the ellipse at $\mathbf{X}(i-1)$ and the inverse image of the major axis of the ellipse at $\mathbf{X}(i)$ approximate the stable and unstable directions at $\mathbf{X}(i-1)$. We note that typically the stable and unstable directions are not orthogonal to each other, and in rare situations they can be identical (Lai et al., 1993b) (nonhyperbolic dynamical systems).

To calculate these stable and unstable directions, we use an algorithm developed in Lai et al., 1993b. This algorithm can be applied to cases where

the period of the orbit is arbitrarily l
$\mathbf{X}$, we first iterate this point forward
trajectory $\mathbf{F}^1(\mathbf{X})$, $\mathbf{F}^2(\mathbf{X}), \ldots, \mathbf{F}^N(\mathbf{X})$.
arbitrarily small radius ε at the poir
once, the circle will become an ellips
along the stable direction of the p
ellipse backward, while at the same
order ε. When we iterate the ellipse
very thin with its major axis along
sufficiently large. For a short peric
integer. In practice, instead of using
point $\mathbf{F}^N(\mathbf{X})$, since the Jacobian mat
in the tangent space of $\mathbf{F}$ toward th
vector backward to the point $\mathbf{X}$ by
inverse map at each point on the al
after each multiplication to unit leng
so obtained at $\mathbf{X}$ is a good approxir

Similarly, to find the unstable
backward under the inverse map N
with $j = N, \ldots, 1$. We then choose
this unit vector forward to the poi
multiplying by the Jacobian matri
Jacobian matrix of the forward m
direction.) We rescale the vector to
at point $\mathbf{X}$ is a good approximatior
N is sufficiently large.

The method above is efficient. Fo
and real stable or unstable directions
for chaotic trajectories in the Hénor

Let $\mathbf{e}_{s,i}$ and $\mathbf{e}_{u,i}$ be the stable and
$\mathbf{f}_{u,i}$ be the corresponding contrava
$\mathbf{f}_{u,i}\cdot\mathbf{e}_{u,i} = \mathbf{f}_{s,i}\cdot\mathbf{e}_{s,i} = 1$ and $\mathbf{f}_{u,i}\cdot\mathbf{e}_{s,i} =$
quire that the next iteration of a t
neighborhood about $\mathbf{X}(i)$, fall along

$$[\mathbf{X}_{n+1} - \mathbf{X}(i$$

If we take the dot product of both
obtain the expression for the param

$$\Delta p_n = \frac{\{\mathbf{A}\cdot[\mathbf{X}_n}$$

The general algorithm for contro

natrix, and **B** is a $d \times r$ matrix:

(9)

$(i), p_0$'

$(i), p_0$'

have

$X] \cdot [X_n - X(i, p_0)]$. (10)

s allow us to find a matrix **K** such
The controllability condition and
d in Barreto and Grebogi, 1995b,
es of magnitude less than one,

complete state of the system X_n is
ce, this is unrealistic. The method
a single scalar time series via the
Yorke, 1991; Ott, 1993). We refer
Spano (1990) and Garfinkel et al.,

pects of the higher-dimensional
al case. (We further simplify the
rameter.) A key aspect of higher-
ble and unstable directions at each
ne stable (unstable) directions are
ave) the periodic orbit exponen-
point of the trajectory can be seen
Choose a small circle of radius ε
e written as $dx^2 + dy^2 = \varepsilon^2$ in the
s at $X(i)$. The image of the circle
$c'dy' + Cdy'^2 = 1$, an equation for
n whose origin is at $X(i-1)$. The
ents of the inverse Jacobian matrix
n ellipse means that the distance
) contracts as a result of the map.
der **F** is typically an ellipse at $X(i)$,
erse image of the major axis of the
ajor axis of the ellipse at $X(i-1)$
he ellipse at $X(i)$ approximate the
e note that typically the stable and
ach other, and in rare situations
hyperbolic dynamical systems).
directions, we use an algorithm
m can be applied to cases where

the period of the orbit is arbitrarily large. To find the stable direction at a point **X**, we first iterate this point forward N times under the map **F** and obtain the trajectory $\mathbf{F}^1(\mathbf{X})$, $\mathbf{F}^2(\mathbf{X}), \ldots, \mathbf{F}^N(\mathbf{X})$. Now imagine that we place a circle of arbitrarily small radius ε at the point $\mathbf{F}^N(\mathbf{X})$. If we iterate this circle backward once, the circle will become an ellipse at the point $\mathbf{F}^{N-1}(\mathbf{X})$, with the major axis along the stable direction of the point $\mathbf{F}^{N-1}(\mathbf{X})$. We continue iterating this ellipse backward, while at the same time rescaling the ellipse's major axis to be order ε. When we iterate the ellipse back to the point **X**, the ellipse becomes very thin with its major axis along the stable direction at the point **X**, if N is sufficiently large. For a short period-m orbit, we choose $N = km$ with k an integer. In practice, instead of using a small circle, we take a unit vector at the point $\mathbf{F}^N(\mathbf{X})$, since the Jacobian matrix of the inverse map $\mathbf{F}^{-1}$ rotates a vector in the tangent space of **F** toward the stable direction. Hence we iterate a unit vector backward to the point **X** by multiplying by the Jacobian matrix of the inverse map at each point on the already existing orbit. We rescale the vector after each multiplication to unit length. For sufficiently large N, the unit vector so obtained at **X** is a good approximation to the stable direction at **X**.

Similarly, to find the unstable direction at point **X**, we first iterate **X** backward under the inverse map N times to obtain a backward orbit $\mathbf{F}^{-j}(\mathbf{X})$ with $j = N, \ldots, 1$. We then choose a unit vector at point $\mathbf{F}^{-N}(\mathbf{X})$ and iterate this unit vector forward to the point **X** along the already existing orbit by multiplying by the Jacobian matrix of the map N times. (Recall that the Jacobian matrix of the forward map rotates a vector toward the unstable direction.) We rescale the vector to unit length at each step. The final vector at point **X** is a good approximation to the unstable direction at that point if N is sufficiently large.

The method above is efficient. For instance, the error between the calculated and real stable or unstable directions (Lai et al., 1993b) is on the order of 10^{-10} for chaotic trajectories in the Hénon map if $N = 20$.

Let $\mathbf{e}_{s,i}$ and $\mathbf{e}_{u,i}$ be the stable and unstable directions at $\mathbf{X}(i)$, and let $\mathbf{f}_{s,i}$ and $\mathbf{f}_{u,i}$ be the corresponding contravariant vectors that satisfy the conditions $\mathbf{f}_{u,i} \cdot \mathbf{e}_{u,i} = \mathbf{f}_{s,i} \cdot \mathbf{e}_{s,i} = 1$ and $\mathbf{f}_{u,i} \cdot \mathbf{e}_{s,i} = \mathbf{f}_{s,i} \cdot \mathbf{e}_{u,i} = 0$. To stabilize the orbit, we require that the next iteration of a trajectory point, after falling into a small neighborhood about $\mathbf{X}(i)$, fall along the stable direction at $\mathbf{X}(i+1, p_0)$, namely

$$[\mathbf{X}_{n+1} - \mathbf{X}(i+1, p_0)] \cdot \mathbf{f}_{u,i+1} = 0. \tag{11}$$

If we take the dot product of both sides of (8) with $\mathbf{f}_{u,i+1}$ and use (10), we obtain the expression for the parameter perturbations:

$$\Delta p_n = \frac{\{\mathbf{A} \cdot [\mathbf{X}_n - \mathbf{X}(i, p_0)]\} \cdot \mathbf{f}_{u,i+1}}{-\mathbf{B} \cdot \mathbf{f}_{u,i+1}}. \tag{12}$$

The general algorithm for controlling chaos for two-dimensional maps can

be summarized as follows:

1. Find the desired unstable periodic orbit to be stabilized.
2. Find a set of stable and unstable directions, $\mathbf{e}_s$ and $\mathbf{e}_u$, at each component of the periodic orbit. The set of corresponding contravariant vectors $\mathbf{f}_s$ and $\mathbf{f}_u$ can be found by solving $\mathbf{e}_s \cdot \mathbf{f}_s = \mathbf{e}_u \cdot \mathbf{f}_u = 1$ and $\mathbf{e}_s \cdot \mathbf{f}_u = \mathbf{e}_u \cdot \mathbf{f}_s = 0$.
3. Randomly choose an initial condition, and evolve the system at the parameter value p_0. When the trajectory enters the ε neighborhood of the target periodic orbit, calculate parameter perturbations at each time step according to (12).

The OGY algorithm described above, when generalized to permit the use of more than one control parameter (Barreto and Grebogi, 1995b), allows greater efficiency in both achieving control and maintaining control in the presence of noise. Furthermore the algorithm is not restricted to the control of unstable periodic orbits. It can be applied to stabilizing chaotic trajectories to synchronize two chaotic systems (Lai and Grebogi, 1993, 1994b) or to convert transient chaos into sustained chaos (Lai and Grebogi, 1994a).

It should be noted that the algorithm discussed above applies to invertible maps. In general, dynamical systems that can be described by a set of first-order autonomous differential equations are invertible, and the inverse system is obtained by letting $t \to -t$ in the original set of differential equations. Hence the discrete map obtained on the Poincaré surface of section also is invertible. Most dynamical systems encountered in practice fall into this category. Noninvertible dynamical systems possess very distinct properties from invertible dynamical systems (Chossat and Golubitsky, 1988; Chin, Kan, and Grebogi, 1993). For instance, for two-dimensional noninvertible maps a point on a chaotic attractor may not have a unique stable (unstable) direction. A method for determining all these stable and unstable directions is not known. If one or several such directions at the target unstable periodic orbit can be calculated, the OGY method can in principle be applied to noninvertible systems by forcing a chaotic trajectory to fall on one of the stable directions of the periodic orbit.

11.4 TARGETING AND CHAOS CONTROL IN A MECHANICAL SYSTEM

We have seen that the OGY algorithm assumes that the control perturbations are limited to be small, and hence the algorithm is based on a linearization of the dynamics in the immediate vicinity of the unstable orbit that is to be stabilized. As described above, it is possible to rely on the natural ergodicity of chaos to bring the trajectory into this small region before applying the control. However, in the case of even moderately high-dimensional systems, the

chaotic transients that occur befo
prohibitively long.

If a reasonable global model of
possible to employ a targeting me
times. (If a global model is not ava
using several simultaneous contro
1995b.) Targeting refers to global, n
method by which a chaotic orbit can
attractor. Several such methods ha
1992a, 1992b, 1993; Bollt and Meiss
method that is computationally effic
stelich et al., 1987). When coupled
targeting allows for faster and more

To demonstrate the advantages
rotor system shown in Figure 11.3.
connected rods subject to periodi
sampled immediately after each ki
(Romeiras et al., 1992; Grebogi et

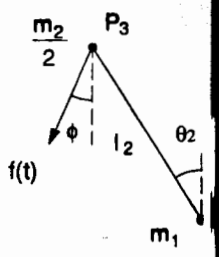

FIGURE 11.3. The kicked double rotor.
stationary point P_1. A second massless r
in turn is mounted at the end of the fi
$\rho_n \delta(t-n)$ are applied at an angle ϕ as sh
the $(n+1)$th kick is given by a four-din
and $\mathbf{Y}_{n+1} = \mathbf{L}\mathbf{Y}_n + \mathbf{G}(\mathbf{X}_{n+1})$ where $\mathbf{X}$ =
nates, $\mathbf{Y} = (\dot{\theta}_1, \dot{\theta}_2)^T$ are the correspondir
function. $\mathbf{M}$ and $\mathbf{L}$ are both constant ma
the two pivots and the moments of ine
parameters at time n are $\rho_n = 9.0 + \delta\rho_n$
set all other parameters to 1. (For furthe
al., 1986, 1987.)

chaotic transients that occur before the control can be applied may be prohibitively long.

If a reasonable global model of the system of interest is available, it is possible to employ a targeting method to effectively reduce these transient times. (If a global model is not available, similar results may be obtained by using several simultaneous control parameters; see Barreto and Grebogi, 1995b.) Targeting refers to global, nonlocal control of chaos; specifically it is a method by which a chaotic orbit can be rapidly steered to a desired part of the attractor. Several such methods have been proposed (Shinbrot et al., 1990, 1992a, 1992b, 1993; Bollt and Meiss, 1995). We describe here a *tree-targeting* method that is computationally efficient for higher-dimensional systems (Kostelich et al., 1987). When coupled with the OGY algorithm described above, targeting allows for faster and more efficient stabilization.

To demonstrate the advantages of this method, we use the kicked double-rotor system shown in Figure 11.3. This is an idealized physical system of two connected rods subject to periodic impulsive kicks. The time evolution, sampled immediately after each kick, is given by a four-dimensional map (Romeiras et al., 1992; Grebogi et al., 1986, 1987). We take our control

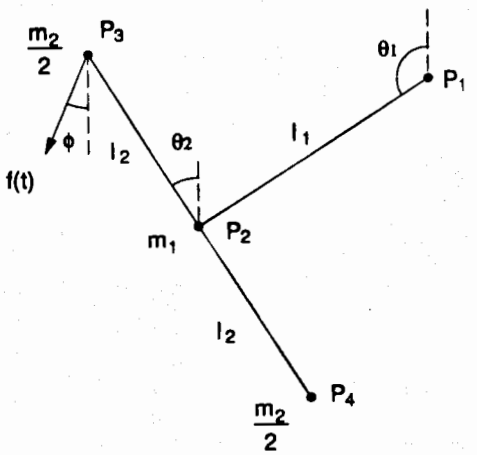

FIGURE 11.3. The kicked double rotor. A massless rod of length l_1 pivots about the stationary point P_1. A second massless rod of length $2l_2$ is mounted on pivot P_2, which in turn is mounted at the end of the first rod. Periodic impulsive kicks $f(t) = \Sigma_{n=0}^{\infty} \rho_n \delta(t - n)$ are applied at an angle ϕ as shown. The state of the system immediately after the $(n + 1)$th kick is given by a four-dimensional map of the form $\mathbf{X}_{n+1} = \mathbf{M}\mathbf{Y}_n + \mathbf{X}_n$ and $\mathbf{Y}_{n+1} = \mathbf{L}\mathbf{Y}_n + \mathbf{G}(\mathbf{X}_{n+1})$ where $\mathbf{X} = (\theta_1, \theta_2)^T$ are the two angular position coordinates, $\mathbf{Y} = (\dot{\theta}_1, \dot{\theta}_2)^T$ are the corresponding angular velocities, and $\mathbf{G}(\mathbf{X})$ is a nonlinear function. $\mathbf{M}$ and $\mathbf{L}$ are both constant matrices that involve the coefficients of friction at the two pivots and the moments of inertia of the rotor. Gravity is absent. Control parameters at time n are $\rho_n = 9.0 + \delta\rho_n$ and $\phi_n = 0.0 + \delta\phi_n$. We take $l_1 = 1/\sqrt{2}$, and set all other parameters to 1. (For further details, see Romeiras et al., 1992; Grebogi et al., 1986, 1987.)

parameters to be the strength of the kick ρ and the angle ϕ at which the kick is applied. Small perturbations ($|\Delta\rho|/\rho_0 \leqslant 0.1$; $|\Delta\phi| \leqslant 0.5$) are applied around nominal values ($\rho_0 = 9.0$, $\phi_0 = 0$) at which the map exhibits 36 fixed points within a chaotic attractor of Lyapunov dimension 2.8 (see the figure caption for further details). This dimension is to be contrasted with most experimental and numerical studies where the dimension was typically between one and two, and often close to one. Figure 11.4 illustrates the advantages of targeting. We seek to stabilize a sequence of five fixed points in succession. The figure displays the θ_1 component of the state versus iteration number. In Figure 11.4*a* we rely on ergodicity to bring the orbit close to the desired fixed point before it is stabilized. In Figure 11.4*b* our tree-targeting method is used. Very large improvements in the switching time is evident; note the great difference in the scales on the two horizontal axes. More precisely, in panel *a* the switching

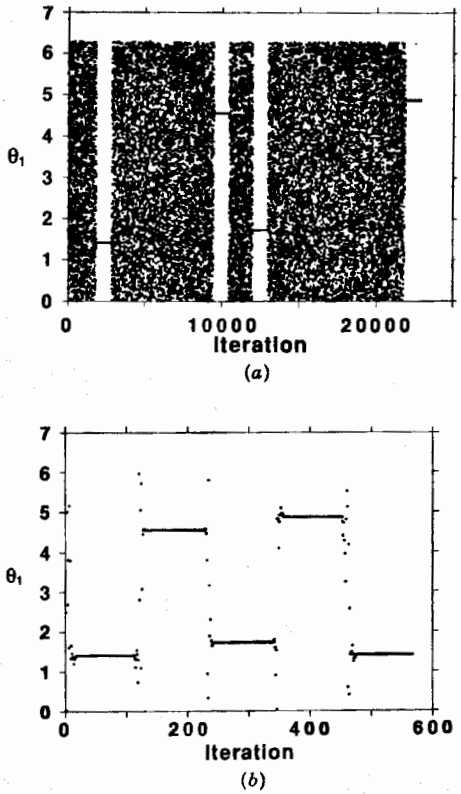

FIGURE 11.4. Graphs illustrating switching between five different fixed points. The θ_1 coordinate of the state is plotted against iteration. (*a*) We rely on ergodicity to bring the orbit close to the desired UPO. The fifth fixed point required 153,485 iterations to be stabilized and is not shown. (*b*) Tree targeting is employed to significantly reduce transients that precede stabilization.

times t follow an exponential dist
chaotic systems (Ott, 1993)), and
iterations to 252,000 ± 3000 iterati
contrast, the method outlined belo
iterations using one parameter tai
parameter targeting (ρ and ϕ). Th
of magnitude in the switching time

The first step in the tree-targetir
periodic orbits that are to be stabili
points, namely periodic orbits of p
For each such point we construc
maps" of the attractor. To stabili
corresponding tree into the vicinity
stabilize the orbit. To switch to $\mathbf{p}_2$
to $\mathbf{p}_2$, and subsequently stabilize t

Each targeting tree is construct
point $\mathbf{p}_1$. The map is then iterat
keeping in memory a short his
consecutive points) until the orb
target. This point, together with t
path of the tree and are stored in r
keeping track of a brief iterate hist
points already in the tree. When th
Continuing in this way, we build a
path is level 1, level 2 branches ar
trunk path, level 3 branches are
objective is to build a tree with en
led chaotic orbit lands near a
iterations.

The basic targeting procedure
target point $\mathbf{t} = \mathbf{x}_{10}$ on the attract
consisting of points $\mathbf{x}_9, \mathbf{x}_8, \ldots, \mathbf{x}_0$ l
Without targeting, the orbit $\mathbf{y}_1, \mathbf{y}_2$
a series of small perturbations to
perturbed orbit $\hat{\mathbf{y}}_1, \hat{\mathbf{y}}_2, \ldots$ lands on
in the path. If this can be accom
will quickly approach the path, a

For specificity, we refer to the
i.e., a four-dimensional map $\mathbf{F}$ wi
exponents). Let S_2 represent the
associated with the point $\mathbf{x}_2$. For s
ρ is available for control. Recall t
single point in $\mathscr{R}^4$. Hence the
$\partial\mathbf{F}(\mathbf{F}(\mathbf{y}_0, \rho_1), \rho_2)/\partial\rho_2$ typically spa
two-dimensional stable manifold

nd the angle ϕ at which the kick
l; $|\Delta\phi| \leq 0.5$) are applied around
the map exhibits 36 fixed points
ension 2.8 (see the figure caption
ontrasted with most experimental
as typically between one and two,
; the advantages of targeting. We
points in succession. The figure
iteration number. In Figure 11.4*a*
to the desired fixed point before
eting method is used. Very large
it; note the great difference in the
ecisely, in panel *a* the switching

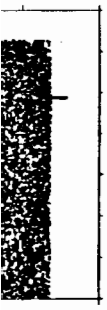

0000

600

een five different fixed points. The θ_1
1. (*a*) We rely on ergodicity to bring
l point required 153,485 iterations to
g is employed to significantly reduce

times t follow an exponential distribution $\langle t\rangle^{-1}\exp(t/\langle t\rangle)$ (this is typical of chaotic systems (Ott, 1993)), and we find that $\langle t\rangle$ ranges from 12,000 $\pm$ 80 iterations to 252,000 $\pm$ 3000 iterations, depending on the fixed point. In sharp contrast, the method outlined below permits the target to be attained in 17–19 iterations using one parameter targeting (ρ), and 13–15 iterations using two parameter targeting (ρ and ϕ). Thus we achieve improvements of 3–4 orders of magnitude in the switching times.

The first step in the tree-targeting procedure is to identify the set of unstable periodic orbits that are to be stabilized. For simplicity, we take these to be fixed points, namely periodic orbits of period one. We denote these by $\mathbf{p}_1, \mathbf{p}_2, \ldots, \mathbf{p}_n$. For each such point we construct *targeting trees*, which function as "road-maps" of the attractor. To stabilize $\mathbf{p}_1$, a chaotic orbit is directed along the corresponding tree into the vicinity of $\mathbf{p}_1$. The OGY method is then applied to stabilize the orbit. To switch to $\mathbf{p}_2$,we can abandon $\mathbf{p}_1$, follow the tree leading to $\mathbf{p}_2$, and subsequently stabilize the orbit there.

Each targeting tree is constructed by first choosing the target, say, the fixed point $\mathbf{p}_1$. The map is then iterated from a random initial condition while keeping in memory a short history of the iterates encountered (e.g., 10 consecutive points) until the orbit lands within a tolerance distance of the target. This point, together with the recorded pre-iterates, comprise the *trunk path* of the tree and are stored in memory. The map is then iterated again, still keeping track of a brief iterate history until the orbit lands near any one of the points already in the tree. When this happens, we add the new path as a *branch*. Continuing in this way, we build a tree with a hierarchy of branches: The trunk path is level 1, level 2 branches are those that are rooted at some point in the trunk path, level 3 branches are rooted at a level 2 branch, and so on. The objective is to build a tree with enough branches such that a typical uncontrolled chaotic orbit lands near a point in the tree after a small number of iterations.

The basic targeting procedure is illustrated in Figure 11.5. Assume that a target point $\mathbf{t} = \mathbf{x}_{10}$ on the attractor has been selected, and that the trunk path consisting of points $\mathbf{x}_9, \mathbf{x}_8, \ldots, \mathbf{x}_0$ has been recorded. Let $\mathbf{y}_0$ be a point near $\mathbf{x}_0$. Without targeting, the orbit $\mathbf{y}_1, \mathbf{y}_2, \ldots$, quickly diverges from the path. We seek a series of small perturbations to available control parameters such that the perturbed orbit $\hat{\mathbf{y}}_1, \hat{\mathbf{y}}_2, \ldots$ lands on the stable manifold of a subsequent point $\mathbf{x}_i$ in the path. If this can be accomplished for a small value of i, then the orbit will quickly approach the path, and $\hat{\mathbf{y}}_{10}$ will be very close to the target $\mathbf{x}_{10}$.

For specificity, we refer to the case of the kicked double rotor (Figure 11.3, i.e., a four-dimensional map $\mathbf{F}$ with two positive and two negative Lyapunov exponents). Let S_2 represent the (typically two-dimensional) stable manifold associated with the point $\mathbf{x}_2$. For simplicity we assume that only one parameter ρ is available for control. Recall that two two-planes generically intersect at a single point in $\mathscr{R}^4$. Hence the vectors $\mathbf{g}_1 = \partial\mathbf{F}(\mathbf{F}(\mathbf{y}_0, \rho_1), \rho_2)/\partial\rho_1$ and $\mathbf{g}_2 = \partial\mathbf{F}(\mathbf{F}(\mathbf{y}_0, \rho_1), \rho_2)/\partial\rho_2$ typically span a two-plane through $\mathbf{y}_2$ that intersects the two-dimensional stable manifold S_2 at a unique point $\hat{\mathbf{y}}_2$. Therefore we look

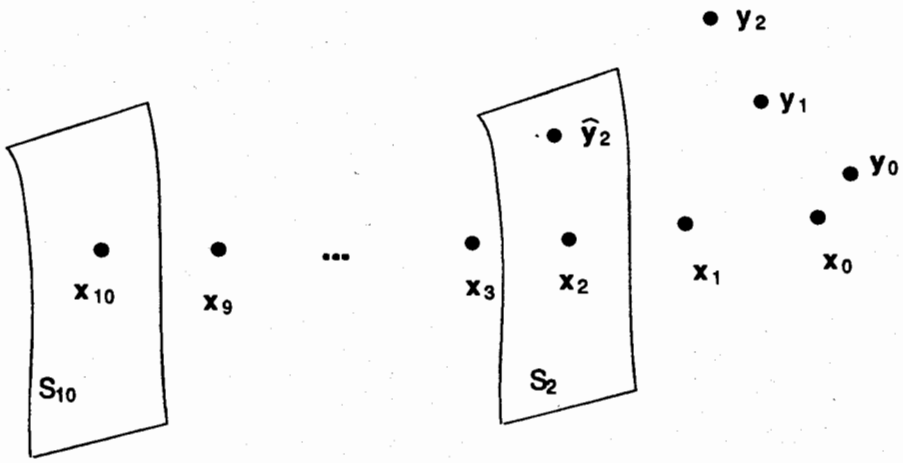

FIGURE 11.5. Schematic of a targeting procedure. Two successive perturbations of the kick are applied at y_0 to steer it onto the stable manifold associated with the point x_2.

for two successive parameter perturbations ρ_1 and ρ_2 such that $\hat{\mathbf{y}}_2$ lies on S_2.

The intersection point $\hat{\mathbf{y}}_2$ may not be sufficiently close to $\mathbf{x}_2$ to justify using the linear approximation for estimating S_2. This is generally the case in our kicked double-rotor example. Alternatively, we can estimate the intersection point on S_2 by calculating the inverse images of points near subsequent points further down the path. Let $\mathbf{s}_1$ and $\mathbf{s}_2$ denote vectors that span a plane at $\mathbf{x}_8$. A point $\mathbf{z} = \mathbf{x}_8 + \sigma_1\mathbf{s}_1 + \sigma_2\mathbf{s}_2$ is chosen with σ_1 and σ_2 small (typically of order 10^{-6}). The inverse images $\mathbf{F}^{-1}(\mathbf{z})$, $\mathbf{F}^{-2}(\mathbf{z}),\ldots$ rapidly approach the stable manifolds S_7, $S_6,\ldots$ because, under the inverse map, S_8 is an expanding set and components perpendicular to S_8 contract.

Thus in the case of one parameter control, we calculate two parameter perturbations ρ_1 and ρ_2, together with values for σ_1 and σ_2, such that

$$\mathbf{F}^{-k}(\mathbf{x}_{k+2} + \sigma_1\mathbf{s}_1 + \sigma_2\mathbf{s}_2) = \mathbf{F}(\mathbf{F}(\mathbf{y}_0, \rho_1), \rho_2) = \hat{\mathbf{y}}_2. \tag{13}$$

In our example, we use $k = 6$. Equation (13) can be solved numerically using Newton's method. Once the prescribed kicks ρ_1 are ρ_2 are applied at $\mathbf{y}_0$ and $\hat{\mathbf{y}}_1$, the orbit lands on the stable manifold of $\mathbf{x}_2$ (at $\hat{\mathbf{y}}_2$), and subsequent iterations of the map approach the path exponentially.

In practice, values of k which yield numerically accurate results can be determined by performing numerical trials on the particular map being considered. To correct for these and other nonideal effects such as noise, state measurement error, and an imperfect determination of the system parameters, the method is reapplied at every iteration.

If two parameters ρ and ϕ are available for control, then only one perturbation step is necessary: Typically there is a two-plane through $\mathbf{y}_1$

spanned by $\mathbf{g}_\rho = \partial\mathbf{F}(\mathbf{y}_0, \rho, \phi)/\partial\rho$ an
stable manifold S_1 of $\mathbf{x}_1$. The pr
extended to different dimensions an
exponents.

Assume now that a three-level tar
can be iterated until the trajectory la
Suppose that $\mathbf{x}$ is in a level 3 branc
interim target, and the orbit is direc
Next we set the interim target to b
The orbit is steered to this new tar
final target is attained. The orbit
applying the OGY control procedu

In the procedure described above
uncontrolled orbit encounters the
cloud of points by calculating the ir
perturbation (applied to ρ) and rep
the cloud are within one iteration
forward a certain number of tim
encounters the tree, its position is
from the initial condition $\mathbf{z}$ onto th
select the path that ultimately rea
iterations.

11.5 CONCLUSIONS

In summary, we have presented
periodic motion by using only sm
takes advantage of chaos and thus
to the system of interest. We hav
suitable for higher-dimensional sy
chaotic transients that precede stab
profound impact on material proc

ACKNOWLEDGMENTS

This work was supported by DOI
Energy Research). In addition E.
Science Consortium under the spo

REFERENCES

Auerbach, D., Grebogi, C., Ott, E., et
systems. *Phys. Rev. Lett.* **69**:3479–3

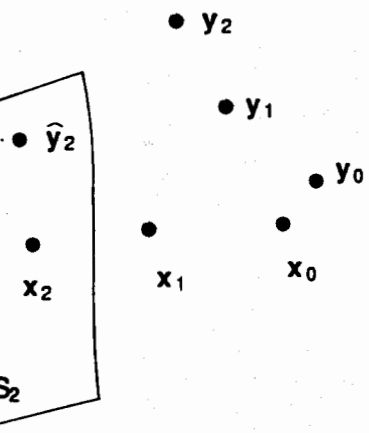

Two successive perturbations of the
nifold associated with the point x_2.

and ρ_2 such that $\hat{\mathbf{y}}_2$ lies on S_2.
ently close to $\mathbf{x}_2$ to justify using
his is generally the case in our
e can estimate the intersection
f points near subsequent points
ctors that span a plane at $\mathbf{x}_8$. A
and σ_2 small (typically of order
. rapidly approach the stable
map, S_8 is an expanding set and

l, we calculate two parameter
for σ_1 and σ_2, such that

$$(\mathbf{y}_0, \rho_1), \rho_2) = \hat{\mathbf{y}}_2. \qquad (13)$$

an be solved numerically using
ρ_1 are ρ_2 are applied at $\mathbf{y}_0$ and
of $\mathbf{x}_2$ (at $\hat{\mathbf{y}}_2$), and subsequent
entially.
rically accurate results can be
on the particular map being
ideal effects such as noise, state
ation of the system parameters,

e for control, then only one
re is a two-plane through $\mathbf{y}_1$

spanned by $\mathbf{g}_\rho = \partial \mathbf{F}(\mathbf{y}_0, \rho, \phi)/\partial\rho$ and $\mathbf{g}_\phi = \partial \mathbf{F}(\mathbf{y}_0, \rho, \phi)/\partial\phi$ that intersects the stable manifold S_1 of $\mathbf{x}_1$. The procedure outlined above can be similarly extended to different dimensions and different numbers of positive Lyapunov exponents.

Assume now that a three-level targeting tree has been constructed. The map can be iterated until the trajectory lands at a point $\mathbf{y}$ near a point $\mathbf{x}$ in the tree. Suppose that $\mathbf{x}$ is in a level 3 branch. The base of this branch is chosen as an interim target, and the orbit is directed there by the method described above. Next we set the interim target to be the root of the adjoining level 2 branch. The orbit is steered to this new target, and the process is repeated until the final target is attained. The orbit is then stabilized at the fixed point by applying the OGY control procedure.

In the procedure described above, an initial condition $\mathbf{z}$ is iterated until the uncontrolled orbit encounters the tree. Another possibility is to generate a cloud of points by calculating the image of $\mathbf{z}$ under a small random parameter perturbation (applied to ρ) and repeating this many times. Thus all points in the cloud are within one iteration of $\mathbf{z}$. This entire cloud can then be iterated forward a certain number of times, and each time a point in the cloud encounters the tree, its position is recorded. In this way many different paths from the initial condition $\mathbf{z}$ onto the tree can be found, and from these we can select the path that ultimately reaches the target in the fewest number of iterations.

11.5 CONCLUSIONS

In summary, we have presented an algorithm for converting chaos into periodic motion by using only small parameter perturbations. This method takes advantage of chaos and thus avoids the need to make large-scale changes to the system of interest. We have also described a global control method suitable for higher-dimensional systems that efficiently reduces the length of chaotic transients that precede stabilization. These methods promise to have a profound impact on material processing and manufacturing.

ACKNOWLEDGMENTS

This work was supported by DOE (Office of Scientific Computing, Office of Energy Research). In addition E. B. was supported by the National Physical Science Consortium under the sponsorship of Argonne National Laboratory.

REFERENCES

Auerbach, D., Grebogi, C., Ott, E., et al. 1992. Controlling chaos in high-dimensional systems. *Phys. Rev. Lett.* **69**:3479–3482.

Barreto, E., Kostelich, E. J., Grebogi, C., et al. 1995a. Efficient switching between controlled unstable periodic orbits in higher dimensional chaotic systems. *Phys. Rev. E* **51**:4169–4172.

Barreto, E., and Grebogi, C. 1995b. Multiparameter control of chaos. *Phys. Rev. E* **52**:3553–3557.

Bielawski, S., Bouazaoui, M., Derozier, D., et al. 1993. Experimental characterization of unstable periodic orbits by controlling chaos. *Phys. Rev. A* **47**:3276–3279.

Bielawski, S., Derozier, D., and Glorieux, P. 1994. Controlling unstable periodic orbits by a delayed continuous feedback. *Phys. Rev. E* **49**:R971–R794.

Bollt, E., and Meiss, J. D. 1995. Controlling chaotic transport through recurrence. *Physica D* **81**:280–294.

Chin, W., Kan, I., and Grebogi, C. 1993. Evolution of attractor boundaries in two-dimensional noninvertible maps. *Random Comp. Dynamics* **1**:349–370.

Chossat, P., and Golubitsky, M. 1988. Symmetry-increasing bifurcation of chaotic attractors. *Physica D* **32**:423–436.

Daw, C. S., Finney, C. E. A., Vasudevan, M., et al. 1995. Self-organization and chaos in a fluidized bed. *Phys. Rev. Lett.* **75**:2308–2311.

Ditto, W. L., Rauseo, S. N., and Spano, M. L. 1990. Experiment control of chaos. *Phys. Rev. Lett.* **65**:3211–3214.

Dressler, U., and Nitsche, G. 1992. Controlling chaos using time delay coordinates. *Phys. Rev. Lett.* **68**:1–4.

Feigenbaum, M. J. 1978. Quantitative university for a class of nonlinear transformations. *J. Stat. Phys.* **19**:25–52.

Garfinkel, A., Spano, M. L., Ditto, W. L., et al. 1992. Controlling cardiac chaos. *Science* **257**:1230–1235.

Gauthier, D. J., Sukow, D. W., Concannon, H. M., et al. 1994. Stabilizing unstable periodic orbits in a fast diode resonator using continuous time-delay autosynchronization. *Phys. Rev. E* **50**:2343–2346.

Gills, Z., Iwata, C., Roy, R., et al. 1992. Tracking unstable steady states: Extending the stability regime of a multimode laser system. *Phys. Rev. Lett.* **69**:3169–3172.

Grebogi, C., Kostelich, E., Ott, E., et al. 1986. Multi-dimensional intertwined basin boundaries and the kicked double rotor. *Phys. Lett. A* **118**:448–452; Erratum (1987) **120A**:497.

Grebogi, C., Kostelich, E. Ott, E., et al. 1987. Multi-dimensional intertwined basin boundaries: Basin structure of the kicked double rotor. *Physica D* **25**:347–360.

Hayes, S., Grebogi, C., and Ott, E. 1993. Communicating with chaos. *Phys. Rev. Lett.* **70**:3031–3034.

Hayes, S., Grebogi, C., Ott, E., et al. 1994. Experimental control of chaos for communication. *Phys. Rev. Lett.* **73**:1781–1784.

Hübinger, B., Doerner, R., Martienssen, W., et al. 1994. Controlling chaos experimentally in systems exhibiting large effective Lyapunov exponents. *Phys. Rev. E* **50**:932–948.

Hunt, E. R. 1991. Stabilizing high-period orbits in a chaotic system: The diode resonator. *Phys. Rev. Lett.* **67**:1953–1955.

Johnson, G. A., and Hunt, E. R. 1993. Controlling in a simple autonomous system: Chua's circuit. *Int. J. Bifurcation Chaos* **3**:789–792.

Kostelich, E., Grebogi, C., Ott, E., et al. *E* **47**:305–310.

Lai, Y. C., and Grebogi, C. 1993. Synch *Phys. Rev. E* **47**:2357–2360.

Lai, Y. C., and Grebogi, C. 1994a. Con feedback control. *Phys. Rev. E* **49**:10

Lai, Y. C., and Grebogi, C. 1994b. Syn by feedback control. *Phys. Rev. E* **50**

Lai, Y. C., Ding, M., and Grebogi, C. 19 *E* **47**:86–92.

Lai, Y. C., Grebogi, C., Yorke, J. A., nonhyperbolic. *Nonlinearity* **6**:779–7

Lai, Y. C., Tél, T., and Grebogi, C. 1 using control. *Phys. Rev. E* **48**:709–7

Meucci, R., Gadomski, W., Ciofini, M., means of weak parametric perturbat

Moon, F. C., Johnson, M. A., and Holn oscillator. *Int. J. Bifurcation Chaos* **6**

Ogata, K. 1987. *Discrete-Time Control*

Ott, E. 1993. *Chaos in Dynamical Syste*

Ott, E., Grebogi, C., and Yorke, J. **64**:1196–1199.

Petrov, V., Crowley, M. J., and Showal in the Belousoc-Zhabotinsky reactio

Petrov, V., Gaspar, V., Masare, J., et Zhabotinsky reaction. *Nature* **361**:2

Reyl, C., Flepp, L., Badii, R., et al. dimensional embedding space. *Phys.*

Rhode, M. A., Rollins, R. W., Markw model of thermal pulse combustion.

Romeiras, F. J., Grebogi, C., Ott, E., et *Physica D* **58**:165–192.

Roy, R., Murphy, T. W., Maier, T. D., e Experimental stabilization of a glob 1262.

Sauer, T., Casdagli, M., and Yorke, J. *A*

Schiff, S. J., Jerger, K., Duong, D. H., et **370**:615–620.

Shinbrot, T., Ott, E., Grebogi, C., et targets. *Phys. Rev. Lett.* **65**:3215–32

Shinbrot, T., Ott, E., Grebogi, C., et al in systems describable by a one-dim

1995a. Efficient switching between
ensional chaotic systems. *Phys. Rev.*

ter control of chaos. *Phys. Rev. E*

3. Experimental characterization of
ys. Rev. A 47:3276–3279.
Controlling unstable periodic orbits
49:R971–R794.
otic transport through recurrence.

lution of attractor boundaries in
mp. Dynamics 1:349–370.
-increasing bifurcation of chaotic

995. Self-organization and chaos in

Experiment control of chaos. *Phys.*

aos using time delay coordinates.

or a class of nonlinear transform-

Controlling cardiac chaos. *Science*

., et al. 1994. Stabilizing unstable
ntinuous time-delay autosynchron-

stable steady states: Extending the
s. Rev. Lett. 69:3169–3172.
ulti-dimensional intertwined basin
tt. A 118:448–452; Erratum (1987)

ulti-dimensional intertwined basin
rotor. *Physica D* 25:347–360.
cating with chaos. *Phys. Rev. Lett.*

perimental control of chaos for

994. Controlling chaos experimen-
v exponents. *Phys. Rev. E* 50:932–

in a chaotic system: The diode

in a simple autonomous system:
2.

Kostelich, E., Grebogi, C., Ott, E., et al. 1993. Higher-dimensional targeting. *Phys. Rev. E* **47**:305–310.

Lai, Y. C., and Grebogi, C. 1993. Synchronization of chaotic trajectories using control. *Phys. Rev. E* **47**:2357–2360.

Lai, Y. C., and Grebogi, C. 1994a. Converting transient chaos into sustained chaos by feedback control. *Phys. Rev. E* **49**:1094–1098.

Lai, Y. C., and Grebogi, C. 1994b. Synchronization of spatiotemporal chaotic systems by feedback control. *Phys. Rev. E* **50**:1894–1899.

Lai, Y. C., Ding, M., and Grebogi, C. 1993a. Controlling Hamiltonian chaos. *Phys. Rev. E* **47**:86–92.

Lai, Y. C., Grebogi, C., Yorke, J. A., et al. 1993b. How often are chaotic saddles nonhyperbolic. *Nonlinearity* **6**:779–797.

Lai, Y. C., Tél, T., and Grebogi, C. 1993c. Stabilizing chaotic-scattering trajectories using control. *Phys. Rev. E* **48**:709–717.

Meucci, R., Gadomski, W., Ciofini, M., et al. 1994. Experimental control of chaos by means of weak parametric perturbations. *Phys. Rev. E* **49**:R2528–R2531.

Moon, F. C., Johnson, M. A., and Holmes, W. T. 1996. Controlling chaos in a two-well oscillator. *Int. J. Bifurcation Chaos* **6**:337–347.

Ogata, K. 1987. *Discrete-Time Control Systems.* Prentice Hall, Englewood Cliffs, NJ.

Ott, E. 1993. *Chaos in Dynamical Systems.* Cambridge University Press, Cambridge.

Ott, E., Grebogi, C., and Yorke, J. A. 1990. Controlling chaos, *Phys. Rev. Lett.* **64**:1196–1199.

Petrov, V., Crowley, M. J., and Showalter, K. 1994. Tracking unstable periodic orbits in the Belousoc-Zhabotinsky reaction. *Phys. Rev. Lett.* **72**:2955–2958.

Petrov, V., Gaspar, V., Masare, J., et al. 1993. Controlling chaos in the Belousov-Zhabotinsky reaction. *Nature* **361**:240–243.

Reyl, C., Flepp, L., Badii, R., et al. 1993. Control of NMR-laser chaos in high-dimensional embedding space. *Phys. Rev. E* **47**:267–272.

Rhode, M. A., Rollins, R. W., Markworth, A. J., et al. 1995. Controlling chaos in a model of thermal pulse combustion. *J. Appl. Phys.* **78**:2224–2232.

Romeiras, F. J., Grebogi, C., Ott, E., et al. 1992. Controlling chaotic dynamical systems. *Physica D* **58**:165–192.

Roy, R., Murphy, T. W., Maier, T. D., et al. 1992. Dynamical control of a chaotic laser: Experimental stabilization of a globally coupled system. *Phys. Rev. Lett.* **68**:1259–1262.

Sauer, T., Casdagli, M., and Yorke, J. A. 1991. Embedology. *J. Stat. Phys.* **65**:579–616.

Schiff, S. J., Jerger, K., Duong, D. H., et al. 1994. Controlling chaos in the brain. *Nature* **370**:615–620.

Shinbrot, T., Ott, E., Grebogi, C., et al. 1990. Using chaos to direct trajectories to targets. *Phys. Rev. Lett.* **65**:3215–3218.

Shinbrot, T., Ott, E., Grebogi, C., et al. 1992a. Using chaos to direct orbits to targets in systems describable by a one-dimensional map. *Phys. Lett. A* **45**:4165–4168.

Shinbrot, T., Ditto, W., Grebogi, C., et al. 1992b. Using the sensitive dependence of chaos (the "butterfly effect") to direct trajectories in an experimental chaotic system. *Phys. Rev. Lett.* **68**:2863–2866.

Shinbrot, T., Grebogi, C., Ott, E., et al. 1993. Using small perturbations to control chaos. *Nature* **363**:411–417.

So, P., and Ott, E. 1995. Controlling chaos using time delay coordinates via stabilization of periodic orbits. *Phys. Rev. E* **51**:2955–2962.

Starrett, J., and Tagg, R. 1994. Control of a chaotic parametrically driven pendulum. *Phys. Rev. Lett.* **74**:1974–1977.

Tél, T. 1991. Controlling transient chaos. *J. Phys. A.* **24**:1359–1368.

EXPER
CONT
HIGH-DI
CH

DAVID J. CHRIST
and PA

The widespread existence of chaoti great interest in the development original feedback chaos control t Yorke (OGY) (Ott et al., 1990) is number of unstable periodic ort attractor. The OGY approach e conditions by making small time systemwide parameter such that t the stable direction of a targeted U an experimental standpoint becau system—all necessary dynamics ar made on the system.

The OGY approach and similar niques have been successfully use systems (Ditto et al., 1990; Hunt, Petrov et al., 1993). However, bec

Dynamics and Chaos in Manufacturing Pro
ISBN 0-471-15293-5